

Electronic Supplementary Information for

Ultrafine ruthenium-iridium-tellurium nanotubes for boosting overall water splitting in acidic media

*Min Liu,^{a,b} Songliang liu,^a Qiqi Mao,^a Shuli Yin,^a Ziqiang Wang,^a You Xu,^a Xiaonian Li,^a Liang Wang^a and Hongjing Wang^{*a}*

^a State Key Laboratory Breeding Base of Green-Chemical Synthesis Technology, College of Chemical Engineering, Zhejiang University of Technology, Hangzhou 310014, P. R. China.

^b Inner Mongolia Key Laboratory of Environmental Chemistry, College of Chemistry and Environmental Science, Inner Mongolia Normal University, Hohhot, Inner Mongolia 010022, P. R. China.

Corresponding author

*E-mail: hjw@zjut.edu.cn (H.W.)

Experimental section

Materials and Chemicals.

RuCl₃, IrCl₃, Na₂TeO₃, NH₃·H₂O (25%-28%), N₂H₄·H₂O (98%), poly(vinylpyrrolidone) (PVP, Mw = 58000), acetone, ethanol, isopropanol, ethylene glycol (EG) and H₂SO₄ were purchased from Aladdin. IrO₂, Commercial Pt/C (20 wt% Pt) was obtained from Alfa Aesar. and Nafion solution (5wt%) were bought from Sigma-Aldrich.

Synthesis of RuIrTe NTs.

Te NWs were firstly synthesized according to the previously reported method.¹ Freshly prepared Te NWs (5 mg) were dissolved with 30 mL of EG in a round-bottom flask under stirring, and then 2 mL of RuCl₃ solution (0.04 M) was added and stirred well. The mixture was subsequently heated in an oil bath at 190 °C for 1 h with reflux. Later, 2 mL of IrCl₃ solution (0.04 M) continued to be added, the mixture was heated in an oil bath at 190 °C for 1 h. The products were centrifuged and washed three times with distilled water and ethanol. The obtained RuIrTe NTs were dispersed in water for further use. The RuTe NTs and IrTe NTs were synthesized by similar procedure but without addition of IrCl₃ solution or RuCl₃ solution.

Synthesis of IrRu nanoparticles (NPs).

IrRu NPs were synthesized with some modifications by the previously reported method.² Under vigorous magnetic stirring, 0.875 g of PVP-58000 was dissolved in 26.25 mL of deionized water to form a homogeneous solution at 25 °C. Then, 0.131 g of IrCl₃·xH₂O and 0.091 g of RuCl₃ were dissolved in the above solution, followed by adding 5.86 mL of N₂H₄·H₂O and 2.89 mL of NH₃·H₂O. The mixed solution was transferred to a Teflon-lined autoclave and kept at 180 °C for 18 h. When the reactor was naturally cooled, the obtained precipitate was centrifuged, washed twice with deionized water and ethanol successively, and dried in vacuum at 60 °C for further use.

Characterizations

Scanning electron microscope (SEM) images were obtained on a Zeiss GeminiSEM 500 microscope at 5 kV. Transmission electron microscope (TEM), high-resolution TEM (HR-TEM), high-angle annular dark field-scanning transmission electron microscopy (HAADF-STEM) and energy dispersive X-ray spectroscopy (EDX) mapping images were acquired on a TalosS-FEG microscope at 200 kV. The powder X-ray diffraction (XRD) pattern was obtained using a panalytic X'Pert-PRO X-ray diffractometer under Cu-K α ($\lambda = 0.1542$ nm) radiation. X-ray photoelectron spectroscopy

(XPS) analysis was performed on an Axis Ultra spectrometer (Kratos Analytical) employing a monochromated Al K α X-ray source (1486.7 eV) operated at 15 kV.

Electrochemical measurements

Electrocatalytic measurements were carried out using the standard three-electrode system of the CHI 760E electrochemical workstation. A catalyst-decorated glassy carbon electrode (GCE), an Ag/AgCl electrode and a graphite rod were utilized as the working, reference and counter electrodes, respectively. The catalyst ink was obtained by dissolving 5 mg of RuIrTe NTs in 0.3 mL of isopropanol, 0.6 mL of water and 0.1 mL of Nafion solution (5 wt%) followed by sonication for 5 min. The GCE (3 mm in diameter) was burnished with alumina powder and cleaned with DI water prior to dropping in the catalyst. The potential measured for the Ag/AgCl electrode was converted to the potential for the RHE with the following equation: $E(\text{vs. RHE}) = E^\theta(\text{Ag/AgCl}) + E(\text{vs. Ag/AgCl}) + 0.059 \text{ pH}$. The working electrode was prepared by dropping 5 μL of catalyst ink onto the polished GCE surface and dried in an oven at 50 $^\circ\text{C}$. The overall water splitting test was implemented in a two-electrode system, using catalyst-loaded carbon paper (0.5 mg cm^{-2}) as both anode and cathode. Pt/C + IrO₂ integrated couple was used as a comparison. For the preparation of the working electrode composed of RuIrTe NTs for HER, the working electrode was pre-cycled from 0 V to 0.1 V (vs. RHE) for 50 cycles at 100 mV s^{-1} in 1 M KOH. The polarization curves for HER, OER and the overall water splitting measurement were tested by linear sweep voltammetry (LSV) with a sweep rate of 5 mV s^{-1} . Electrochemical impedance spectroscopy (EIS) investigations were recorded in the frequency ranging from 100 kHz to 1 Hz at -0.057 V for HER and 1.503 V for OER. For iR correction, the uncompensated Ohmic resistance value for the electrode in the electrolyte solution was measured by EIS.

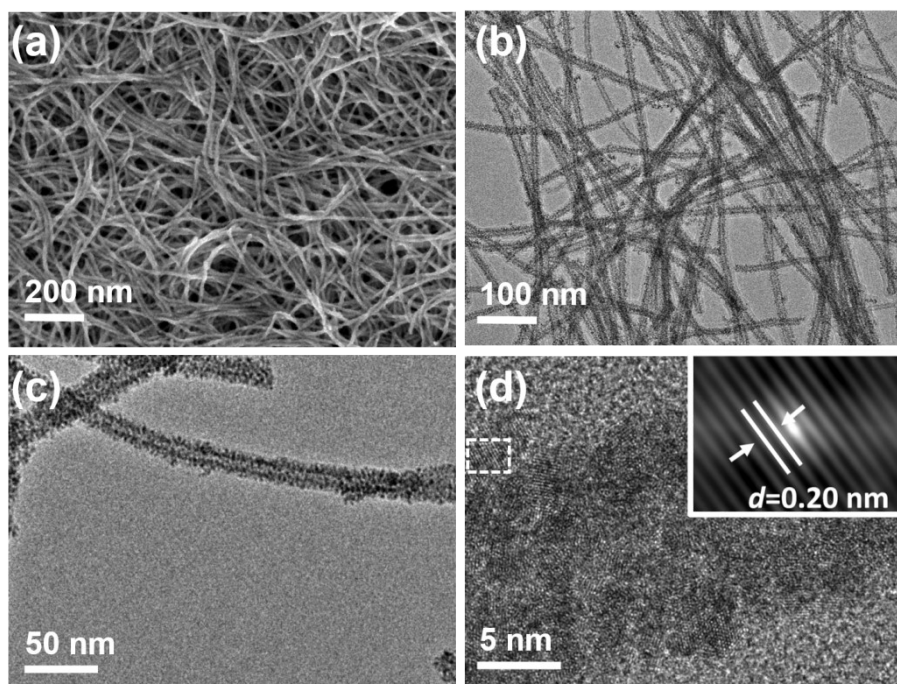


Fig. S1 (a) SEM, (b, c) TEM and (d) HRTEM images of the RuTe NTs. The inset in (d) displays the corresponding Fourier-filtered lattice fringes.

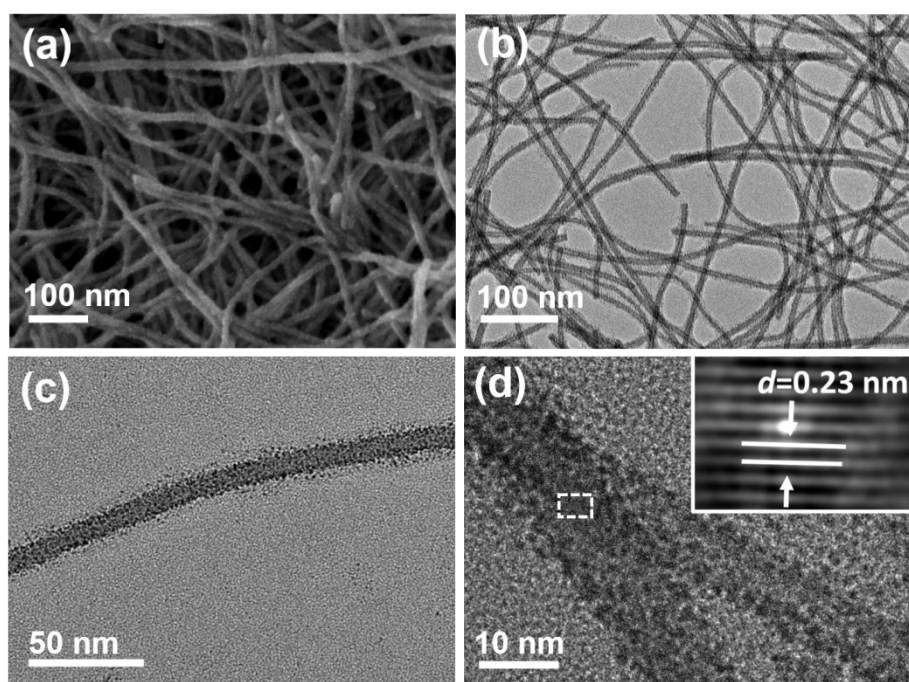


Fig. S2 (a) SEM, (b, c) TEM and (d) HRTEM images of the IrTe NTs. The inset in (d) displays the corresponding Fourier-filtered lattice fringes.

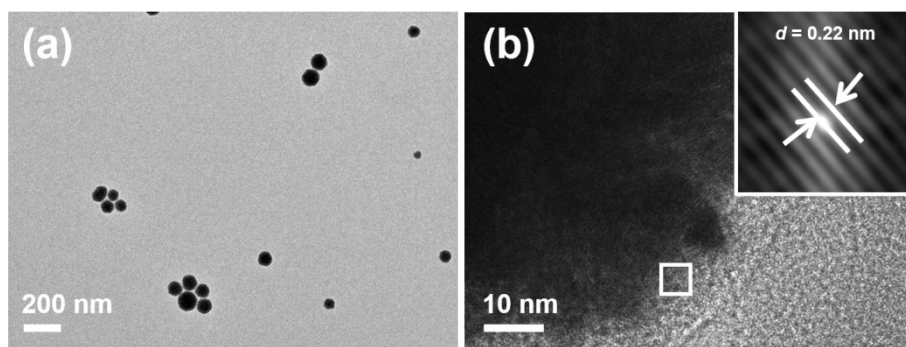


Fig. S3 (a) TEM and (b) HRTEM images of the IrRu NPs. The inset in (b) displays the corresponding Fourier-filtered lattice fringes.

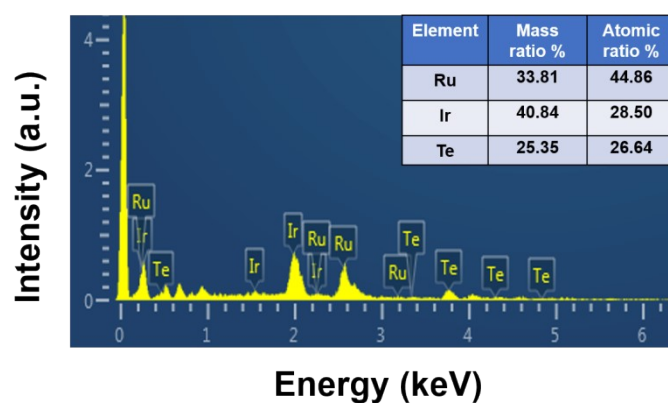


Fig. S4 EDX spectrum of the RuIrTe NTs.

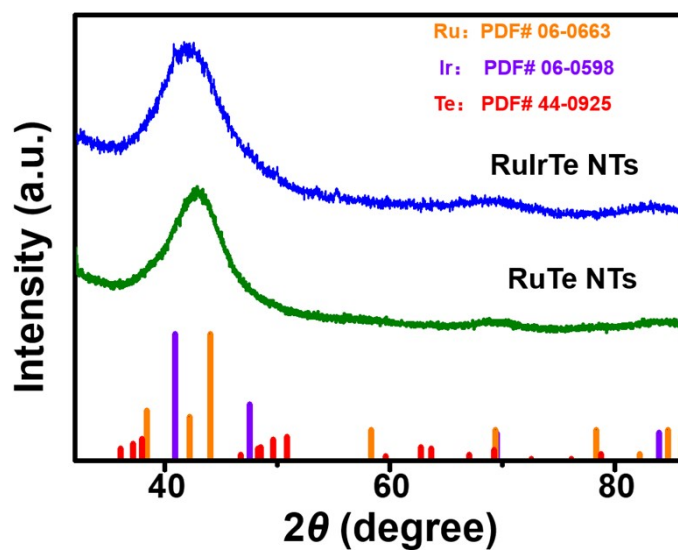


Fig. S5 XRD pattern of the RuIrTe NTs and RuTe NTs.

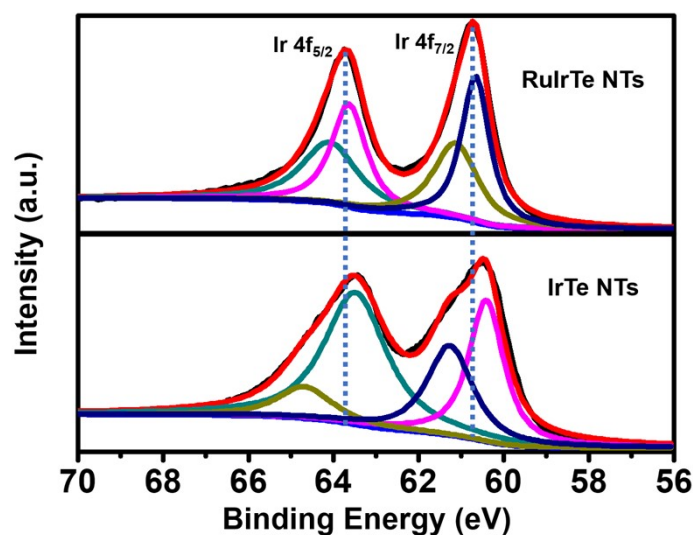


Fig. S6 XPS spectra of Ir 4f for the RuIrTe NTs and IrTe NTs.

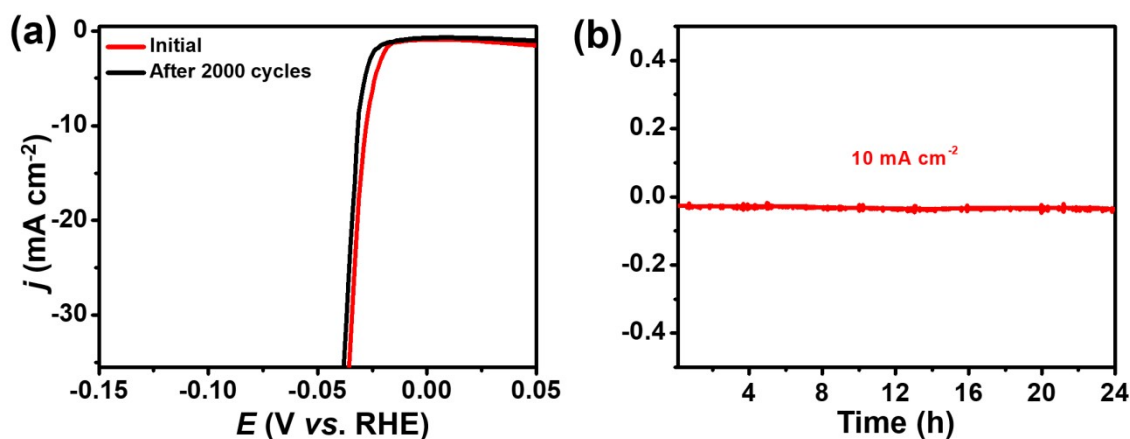


Fig. S7 (a) HER polarization curves (with iR correction) for RuIrTe NTs before and after 2000 CV cycles. (b) The chronopotentiometric curve of RuIrTe NTs with constant cathode-current density of $10 \text{ mA} \cdot \text{cm}^{-2}$ for 24 h in $0.5 \text{ M H}_2\text{SO}_4$.

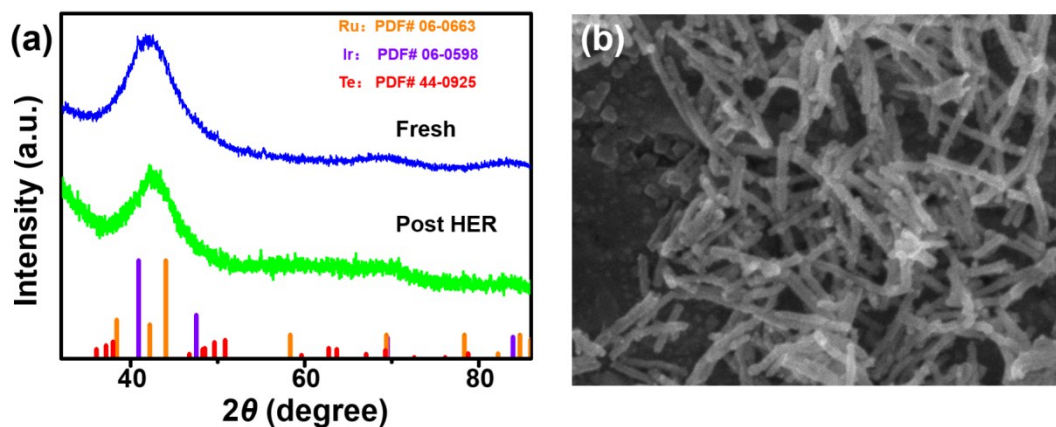


Fig. S8 (a) The XRD pattern of the RuIrTe NTs before and after catalytic stability test. (b) SEM image of the RuIrTe NTs after catalytic stability test.

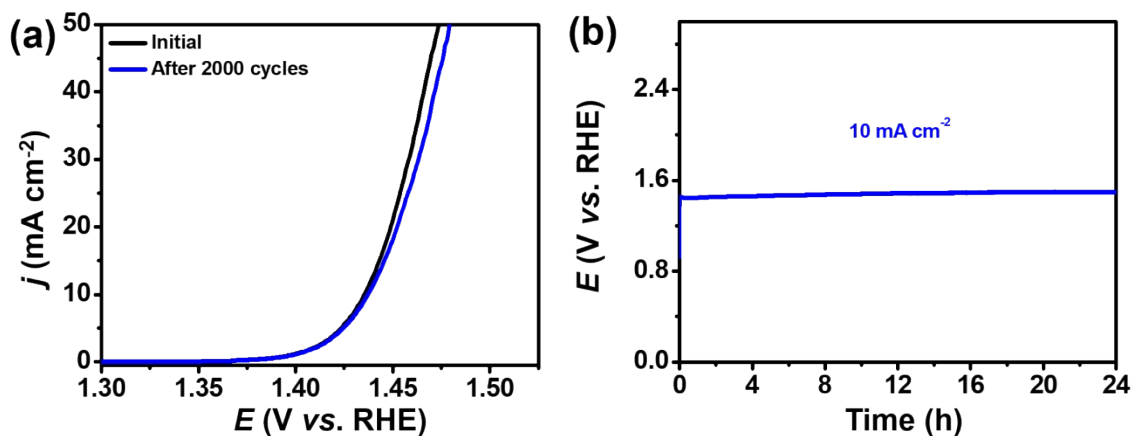


Fig. S9 (a) OER polarization curves (with iR correction) for RuIrTe NTs before and after 2000 CV cycles. (b) The chronopotentiometric curve of RuIrTe NTs with constant anode-current density of 10 mA · cm⁻² for 24 h in 0.5 M H₂SO₄.

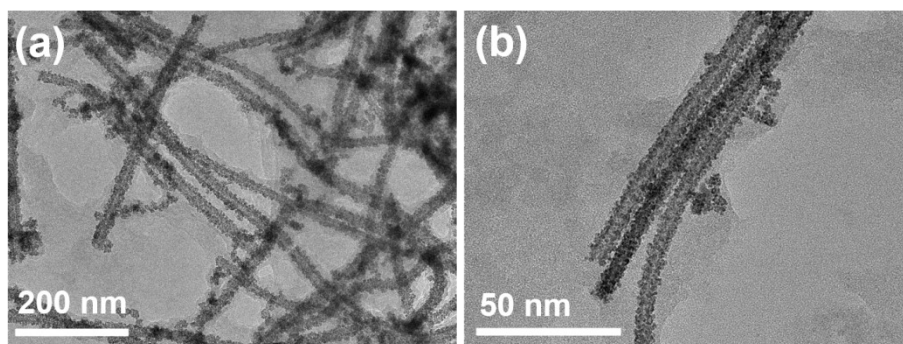


Fig. S10 TEM images of the RuIrTe NTs after long-term stability test.

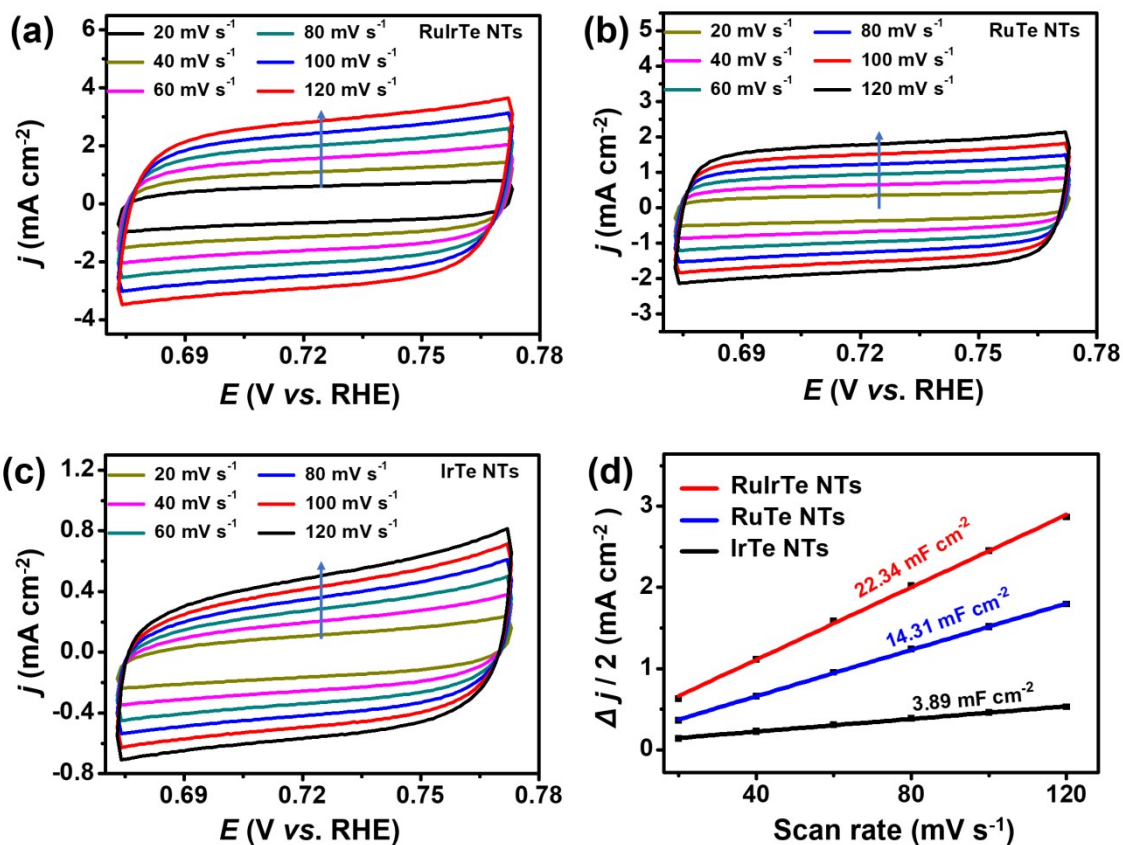


Fig. S11 (a-c) Typical CV curves of RuIrTe NTs, RuTe NTs and IrTe NTs with different scan rates. (d) Capacitive current densities at 0.724 V (vs. RHE) derived from CVs against scan rates for the samples.

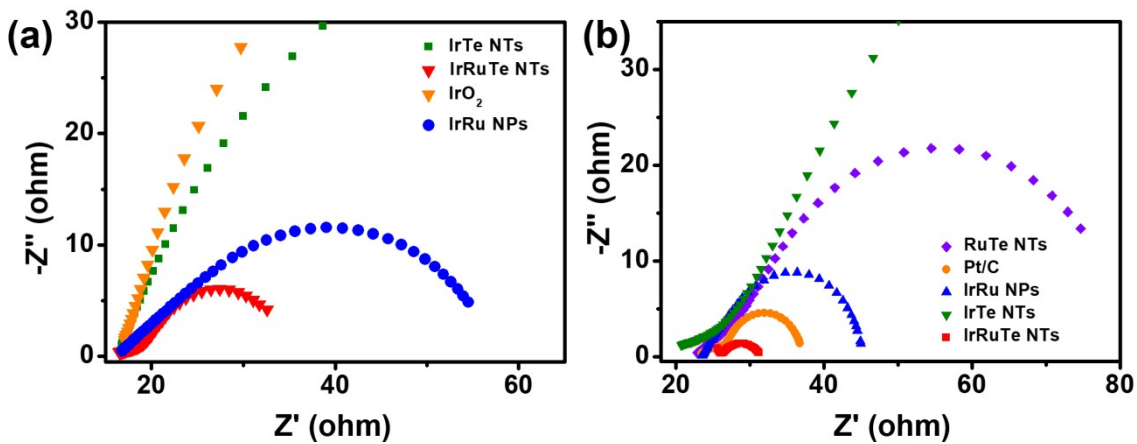


Fig. S12 EIS of various catalysts in 0.5 M H₂SO₄ under applied potentials of (a) 1.503 V and (b) - 0.057 V (vs. RHE).

Table S1. Comparisons of the HER activity for the RuIrTe NTs and some recently reported catalysts.

Catalysts	Electrolyte	Current density	η_{10} (mV)	Ref.
RuIrTe NTs	0.5 M H₂SO₄	10 mA cm⁻²	29	This work
Ru/C ₃ N ₄ /C	0.5 M H ₂ SO ₄	10 mA cm ⁻²	70	3
Ru@WNO-C	0.5 M H ₂ SO ₄	10 mA cm ⁻²	172	4
Rh-MoS ₂	0.5 M H ₂ SO ₄	10 mA cm ⁻²	47	5
CoS/P/CNT	0.5 M H ₂ SO ₄	10 mA cm ⁻²	64	6
nanoisland-rich IrCu NWs	0.5 M H ₂ SO ₄	10 mA cm ⁻²	38	7
RuP ₂ @NPC	0.5 M H ₂ SO ₄	10 mA cm ⁻²	38	8
Ru-MoO ₂	0.5 M H ₂ SO ₄	10 mA cm ⁻²	55	9
Ru ⁰ /CeO ₂	0.5 M H ₂ SO ₄	10 mA cm ⁻²	41	10
Ir-NCNSs	0.5 M H ₂ SO ₄	10 mA cm ⁻²	46.3	11
Ru/MeOH/THF	0.5 M H ₂ SO ₄	10 mA cm ⁻²	83	12

Table S2. Comparisons of the OER activity for the RuIrTe NTs and some recently reported catalysts.

Catalysts	Electrolyte	Current density	η_{10} (mV)	Ref.
RuIrTe NTs	0.5 M H₂SO₄	10 mA cm⁻²	205	This work
nanoisland-rich IrCu NWs	0.5 M H ₂ SO ₄	10 mA cm ⁻²	242	7
Ir-W@Ir-WO _{3-x}	0.5 M H ₂ SO ₄	10 mA cm ⁻²	261	13
IrO ₂ -RuO ₂ @Ru	0.5 M H ₂ SO ₄	10 mA cm ⁻²	281	14
IrRu@Te	0.5 M H ₂ SO ₄	10 mA cm ⁻²	220	2
RuB ₂	0.5 M H ₂ SO ₄	10 mA cm ⁻²	223	15
SrIrO	0.5 M H ₂ SO ₄	10 mA cm ⁻²	245	16
IrO _x -Ir	0.5 M H ₂ SO ₄	10 mA cm ⁻²	290	17
Pt _{0.1} La _{0.1} -IrO ₂ @NC	0.5 M H ₂ SO ₄	10 mA cm ⁻²	205	18
RuNi ₂ @G-250	0.5 M H ₂ SO ₄	10 mA cm ⁻²	227	19
np-IrO ₂	0.5 M H ₂ SO ₄	10 mA cm ⁻²	240	20

Table S3. Comparisons of the overall water splitting performance for the RuIrTe NTs and some recently reported catalysts.

Catalysts	Electrolyte	Voltage at 10 mA cm ⁻² (V)	Ref.
RuIrTe NTs	0.5 M H₂SO₄	1.511	This work
Ir-Ag nanotubes	0.5 M H ₂ SO ₄	1.55	21
Ru NCs/Co ₂ P HMs	0.5 M H ₂ SO ₄	1.53	22
IrNi NCs	0.5 M H ₂ SO ₄	1.58	23
IrCoNi/CFP	0.5 M H ₂ SO ₄	1.56	24
Ir@NG-750	0.5 M H ₂ SO ₄	1.54	25

References

1. H. S. Qian, S. H. Yu, J. Y. Gong, L. B. Luo and L. F. Fei, *Langmuir*, 2006, **22**, 3830-3835.
2. J. Xu, Z. Lian, B. Wei, Y. Li, O. Bondarchuk, N. Zhang, Z. Yu, A. Araujo, I. Amorim and Z. Wang, *ACS Catal.*, 2020, **10**, 3571-3579.
3. Y. Zheng, Y. Jiao, Y. Zhu, L. H. Li, Y. Han, Y. Chen, M. Jaroniec and S.-Z. Qiao, *J. Am. Chem. Soc.*, 2016, **138**, 16174-16181.
4. G. Meng, H. Tian, L. Peng, Z. Ma, Y. Chen, C. Chen, Z. Chang, X. Cui and J. Shi, *Nano Energy*, 2021, **80**, 105531.
5. Y. Cheng, S. Lu, F. Liao, L. Liu, Y. Li and M. Shao, *Adv. Funct. Mater.*, 2017, **27**, 1700359.
6. W. Liu, E. Hu, H. Jiang, Y. Xiang, Z. Weng, M. Li, Q. Fan, X. Yu, E. I. Altman and H. Wang, *Nat. Commun.*, 2016, **7**, 1-9.
7. D. Cao, J. Wang, H. Zhang, H. Xu and D. Cheng, *Chem. Eng. J.*, 2021, **416**, 129128.
8. Z. Pu, I. S. Amiinu, Z. Kou, W. Li and S. Mu, *Angew. Chem., Int. Ed.*, 2017, **56**, 11559-11564.
9. P. Jiang, Y. Yang, R. Shi, G. Xia, J. Chen, J. Su and Q. Chen, *J. Mater. Chem. A*, 2017, **5**, 5475-5485.
10. E. Demir, S. Akbayrak, A. M. Önal and S. Özkar, *ACS Appl. Mater. Interfaces*, 2018, **10**, 6299-6308.
11. X. Wu, Z. Wang, K. Chen, Z. Li, B. Hu, L. Wang and M. Wu, *ACS Appl. Mater. Interfaces*, 2021, **13**, 22448-22456.
12. S. Drouet, J. Creus, V. Collière, C. Amiens, J. García-Antón, X. Sala and K. J. C. C. Philippot, *Chem. Commun.*, 2017, **53**, 11713-11716.
13. Z. Lu, C. Wei, X. Liu, Y. Fang, X. Hao, Y. Zang, Z. Pei, J. Cai, Y. Wu and D. Niu, *J. Mater. Chem. A*, 2021.
14. G. Li, S. Li, J. Ge, C. Liu and W. Xing, *J. Mater. Chem. A*, 2017, **5**, 17221-17229.
15. D. Chen, T. Liu, P. Wang, J. Zhao, C. Zhang, R. Cheng, W. Li, P. Ji, Z. Pu and S. Mu, *ACS Energy Lett.*, 2020, **5**, 2909-2915.
16. L. Zhang, H. Jang, Z. Li, H. Liu, M. G. Kim, X. Liu and J. Cho, *Chem. Eng. J.*, 2021, **419**, 129604.
17. P. Lettenmeier, L. Wang, U. Golla-Schindler, P. Gazdzicki, N. A. Cañas, M. Handl, R. Hiesgen, S. S. Hosseiny, A. S. Gago and K. Friedrich, *Angew. Chem., Int. Ed.*, 2016, **128**, 752-756.

18. S. Hao, Y. Wang, G. Zheng, L. Qiu, N. Xu, Y. He, L. Lei and X. Zhang, *Appl. Catal., B*, 2020, **266**, 118643.
19. X. Cui, P. Ren, C. Ma, J. Zhao, R. Chen, S. Chen, N. P. Rajan, H. Li, L. Yu and Z. Tian, *Adv. Mater.*, 2020, **32**, 1908126.
20. Q. Li, J. Li, J. Xu, N. Zhang, Y. Li, L. Liu, D. Pan, Z. Wang and F. L. Deepak, *ACS Appl. Energy Mater.*, 2020, **3**, 3736-3744.
21. M. Zhu, Q. Shao, Y. Qian and X. Huang, *Nano Energy*, 2019, **56**, 330-337.
22. Y. Deng, L. Yang, Y. Wang, L. Zeng, J. Yu, B. Chen, X. Zhang and W. Zhou, *Chin. Chem. Lett.*, 2021, **32**, 511-515.
23. Y. Pi, Q. Shao, P. Wang, J. Guo and X. Huang, *Adv. Funct. Mater.*, 2017, **27**, 1700886.
24. J. Feng, F. Lv, W. Zhang, P. Li, K. Wang, C. Yang, B. Wang, Y. Yang, J. Zhou and F. Lin, *Adv. Mater.*, 2017, **29**, 1703798.
25. X. Wu, B. Feng, W. Li, Y. Niu, Y. Yu, S. Lu, C. Zhong, P. Liu, Z. Tian and L. Chen, *Nano Energy*, 2019, **62**, 117-126.